

# Optical thin film filters of colloidal gold and silica nanoparticles prepared by a layer-by-layer self-assembly method

Zaheer Abbas Khan · Rachana Kumar ·  
Waleed S. Mohammed · Gabor L. Hornyak ·  
Joydeep Dutta

Received: 7 February 2011 / Accepted: 20 May 2011 / Published online: 4 June 2011  
© Springer Science+Business Media, LLC 2011

**Abstract** A novel fabrication method for optical thin film filters based on the self-organization of alternating layers of colloidal gold and silica nanoparticles (NP) is reported. The filter is designed to work in the deep-UV to visible spectral range. The spectral absorption peaks are tuned by three parameters: the organic capping ligand of the gold NPs (citrate, chitosan, poly (diallyl-dimethylammonium)-chloride or PDDA); the capping environment (bare, chitosan, or PDDA) of the silica NPs and the thickness of the film. Precise control of the transmission color (less than 1% color distance per layer), is achieved by changing the film thickness. Exploitation of the self-assembly process should lead to the facile production of highly reliable large area thin film optical filters at considerably lower costs.

## Introduction

Thin film optical filters can be categorized depending on their construction and mechanism of operation such as dichroic filters, reflective filters, or interference optical filters [1]. Fabry–Perot interferometer is a common thin film filter [2]. The absorption and refractive properties of the metal or the dielectric used in the film can determine

the operation range of the filter in ultraviolet (UV), visible (Vis), or infrared (IR) regions [3, 4]. A combination of several metals and/or dielectrics is used in multilayer structures for designing spectral filters with desired specifications [5]. The spectral characteristics of these filters are a function of the collective properties of individual components of the layered coatings (e.g., transmittance, absorbance, reflectance, density, refractive index, and homogeneity) and their physical configuration (e.g., layer thickness and microstructure). Traditional techniques used for fabricating multilayer thin film optical filters are high vacuum deposition methods like ion-assisted deposition [6], ion-beam sputtering [7], vacuum vapor deposition [8], electron-beam evaporation [9], and reactive ion plating methods [10] among others. Filters fabricated by these processes consist of a few to hundreds of layers of films that require precise control over the deposition of each layer and requires advanced facilities to support the processes.

Self-assembly method offers a novel, inexpensive, bottom-up approach for the fabrication of thin films using multiple layers of nanoparticles (NP)'s [11, 12]. The process is normally conducted at room temperature with versatile and easy to acquire organic–inorganic materials. Dip coating is a common self-assembly technique that involves the sequential exposure of a substrate into alternating cationic and anionic colloidal solutions popularly known as layer-by-layer (LBL) technique [13, 14]. In this study, dip coating technique was utilized to form a thin film optical filter that comprises of multiple bi-layers of gold and silica NPs. The spectral response of the filter is effectively tuned by the capping layer of NPs and the number of layers in the film.

If metal NPs are used in the growth of films, optical absorption would be dominated by the surface plasmon

---

**Electronic supplementary material** The online version of this article (doi:[10.1007/s10853-011-5651-0](https://doi.org/10.1007/s10853-011-5651-0)) contains supplementary material, which is available to authorized users.

---

Z. A. Khan · R. Kumar · G. L. Hornyak · J. Dutta (✉)  
Center of Excellence in Nanotechnology (CoEN),  
Asian Institute of Technology, Bangkok, Thailand  
e-mail: joy@ait.asia

W. S. Mohammed  
School of Engineering, Bangkok University,  
Pathum Thani 12120, Thailand

resonance (SPR) [15]. The resonance depends strongly on particle size [16, 17], shape [18, 19], and the average interparticle distance as well as the nature of the protecting organic shells often used for the stabilization of the NPs if synthesized as colloids [20, 21]. The SPR, and hence the peak absorption, in NPs is due to coherent oscillations of the conduction electrons induced by the electromagnetic field of the incident light [22]. Gold NPs, for example, exhibit a strong absorption band in the visible region of the electromagnetic spectrum [23]. Silica NPs are optically transparent in the visible region and absorb light mostly in the ultraviolet [24]. Therefore, a thin film with multilayers of both gold and silica NPs can be designed as an absorption filter in the spectral range from ultraviolet to visible. If NPs size is held constant and the shape is spherical, then the fundamental tuning parameters of the filter are the particle distribution, metal–ligand interaction and the nature of the dielectric host medium.

In general, the performance of any optical filter depends on the spectrum-selectivity. A good band-rejection filter, which is the focus in this study, significantly reduces power transmission in the desired range of the spectrum with almost 100% transmission everywhere else. As a color filter, it is also desired to precisely control the color with the control parameter.

## Experimental details

### Synthesis and surface modification of gold NPs

Gold NPs were synthesized in an aqueous solution by the reduction of chloroauric acid ( $\text{HAuCl}_4$ ) with trisodium citrate ( $\text{Na}_3\text{C}_6\text{H}_5\text{O}_7$ ) following the well-known method described by Turkevich [25, 26]. This rendered negatively charged citrate-capped gold NPs. The average size of gold NPs obtained by this method was around 20 nm. Gold NPs were also synthesized by addition of chitosan (0.1% solution prepared in 1% acetic acid) for the reduction of chloroauric acid. The chitosan-capped gold NPs yielded a positively charged surface in acidic solution [27]. Capping of gold NPs with poly (diallyl-dimethylammonium)-chloride (PDDA) was done by adding 0.1% solution of PDDA (35 wt% in water) to the citrate-reduced colloidal suspension of gold NPs and stirred for 30 min. PDDA-capped gold NPs also yielded a positively charged surface at acidic pH [28].

### Synthesis and surface modification of silica NPs

The synthesis of silica ( $\text{SiO}_2$ ) NPs by the Stöber method is another well-known process that has been reported extensively [29]. Silica NPs with an average size of 30 nm were

used in this study. As produced silica NPs bear a negative charge due to the surface hydroxyl group. These silica NPs were then capped with PDDA by the addition of 0.1% solution of PDDA (35 wt% in water) to the colloidal suspension of silica NPs and stirred for 30 min. The PDDA-capped silica NPs bear a positive charge due to quaternary amines [30]. Silica NPs were also capped by addition of chitosan solution (0.1% solution prepared in 1% acetic acid) to colloidal suspension of silica NPs. The chitosan-capped silica NPs bear a positive charge at acidic pH [31].

### Filter fabrication using self-assembly technique

This section describes the approach for the fabrication of thin film optical filters by LBL technique by the selection of compatible light absorbing components and tuning SPR shift by application of capping agents as well as by controlling the total number of layers in the films.

The LBL formation is done by an in-house developed automated dip coating system [32]. A schematic representation of the system is presented in Fig. 1. Multiple layers of gold and silica NPs forming the consecutive layers should bear opposite electrical charges. Gold NPs bear negative charge when formed from a gold precursor ( $\text{HAuCl}_4$ ) using trisodium citrate as a reducing agent [33, 34]. Since bare silica NPs in aqueous media carry a negative charge due to hydroxyl ( $\text{OH}^-$ ) group. For forming bi-layers, gold–silica NPs require proper capping with positive charge densities that were achieved by coating with chitosan or PDDA as explained above.

Of the nine possible combinations of Au and silica NPs, only four combinations can form the appropriate positive–negative charge layer required for growing the

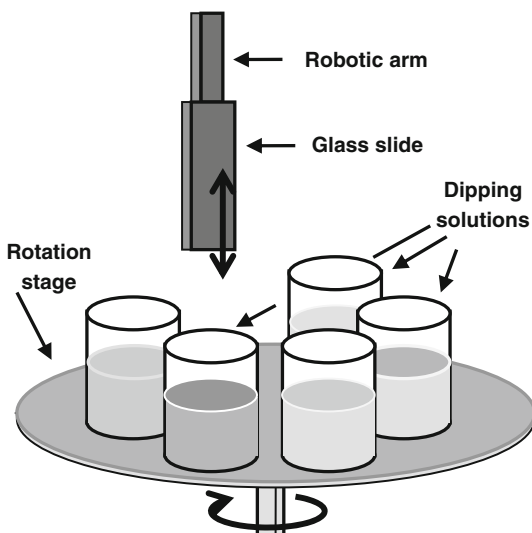


**Fig. 1** Schematic diagram of the LBL automated dip coating system

multilayered films. Microscopic glass slides were used as substrates and cleaned in 1:1 (v/v) MeOH:HCl solution followed by treatment in concentrated H<sub>2</sub>SO<sub>4</sub> to remove surface contaminants and then dried in air in an oven kept at 150 °C. Following this, the substrates were functionalized by APTS (3-aminopropyl trimethoxysilane) to render negative charges on the glass substrates that were used for film deposition [35]. At this stage, a water contact angle of 45° was measured for the glass substrates indicating a hydrophilic surface.

The substrates were immersed into a sequence of different solutions through the vertical movement of the robotic arm holding the substrates and the rotation of the stage carrying the solutions. The solutions used were colloidal gold and silica NPs (with specific cappings), deionised water, acetate buffer, and citrate buffer. The buffer solutions were used to avoid any change in the pH of the colloidal solutions during the dip coating process [36]. In this study, an optimized dipping time of 5 min for the deposition of each layer was used [32]. The process was repeated to deposit the targeted number of layers.

## Results and discussion

The following sections illustrate the tuning of the optical properties using three main parameters: film thickness, silica NPs capping, and gold NPs capping.

The scanning electron micrographs (SEM) of the thin films show that the LBL deposition lead to a stack of individual particulate layers (Fig. 2a). There is a minimum spacing among the NPs (Fig. 2b) due to their random sequential absorption that lowers the final saturation coverage [37, 38].

### Effect of capping on optical filter response

The measured absorption spectra for the four possible layered structures are shown in Fig. 3 (in each case 50 bi-layers were deposited). The absorption coefficient of the film is estimated assuming a uniform layer thickness. The normalized transmittance ' $T$ ' is given by the equation,  $I(\lambda, z) = \text{Exp}[-2\alpha(\lambda)z]$ , where ' $\lambda$ ' is the wavelength, ' $\alpha$ ' is the absorption coefficient, and ' $z$ ' is the film thickness. Figure 3a shows the reduction of the absorption peak of gold (~528 nm) and silica (~330 nm) when capped with PDDA. The trend is the same when capping with chitosan as shown in Fig. 3b.

Chitosan is known to get protonated at dilute acidic conditions (i.e., pH = 4) while the pH of colloidal silica NPs is more toward basic (pH = 8–9) resulting in partial capping. Therefore, less amount of silica NPs are available for electrostatic interaction with gold NPs leading to lower

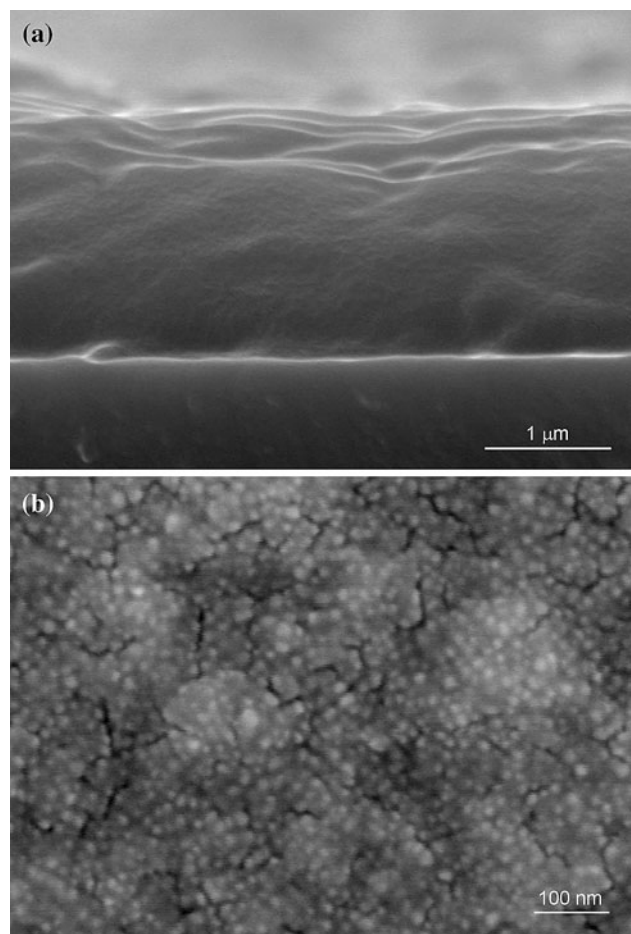


**Fig. 2** **a** SEM (cross section) of 50 bi-layers of chitosan-capped gold and silica. **b** SEM (top) of 100 bi-layers of gold with chitosan-capped silica

volume fraction of silica in the films when polyelectrolyte coated silica was used (Fig. 3a, b).

In retrospect, capping the gold NPs with polyelectrolyte (PDDA or chitosan) results in the reduction of peak value of plasmon absorbance (~525 nm) as shown in Table 1. The deconvolution of the optical absorption spectra for gold NPs showed that it fits into two peaks, one at 522–525 nm corresponding to the transverse plasmon resonance ( $\lambda_P$ ) that is generated due to the dipolar oscillation in the spherical NPs constituting the thin films. The second peak at 552–559 nm is due to the longitudinal plasmon resonance ( $\lambda_{PL}$ ) that appears due to the close proximity of the gold NPs in the film resulting in the electromagnetic interaction among the gold NPs [39, 40]. Table 1 gives the values for Full width at half maximum (FWHM), transverse plasmon wavelength, and longitudinal plasmon wavelength values. In the case of gold capped with PDDA or chitosan, FWHM is higher as compared to uncapped gold due to some agglomeration of the NPs [34].

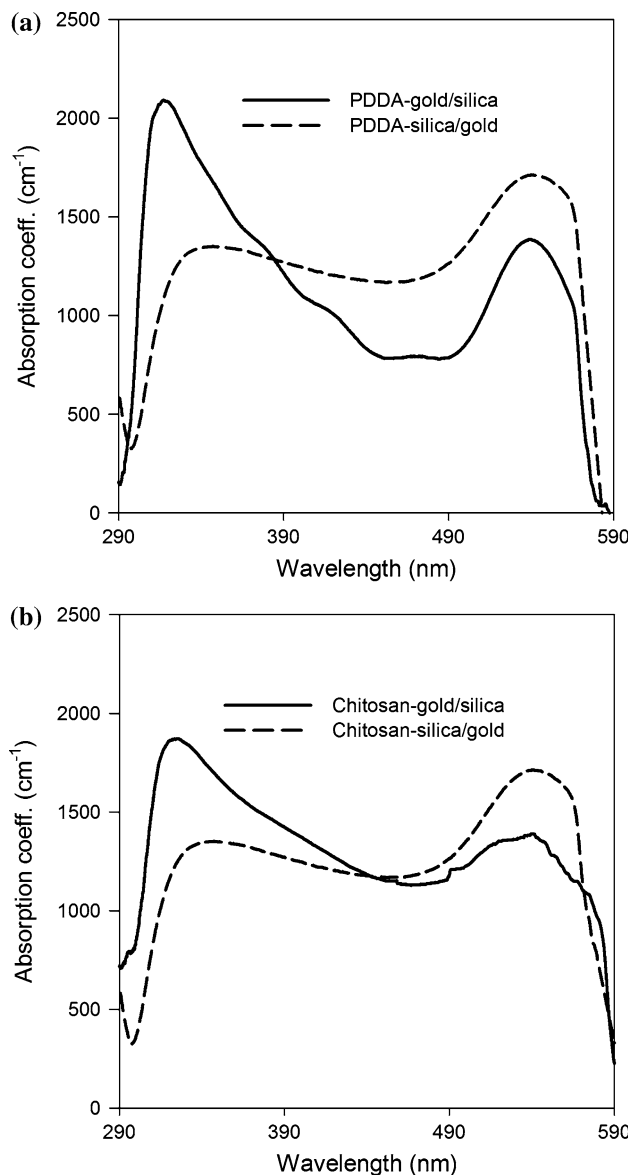


**Fig. 3** Measured absorption coefficient of the film when using two different cappings: **a** PDDA with gold (solid) and silica (dashed) and **b** Chitosan with gold (solid) and silica (dashed)

**Table 1** Measured values of FWHM for absorbance spectra in Fig. 3

	$\lambda_{\text{peak height}}$	$\lambda_P$ (nm)	$\lambda_{\text{PL}}$ (nm)	FWHM (nm)
Uncapped gold	0.65	522	–	35.39
PDDA-capped gold	0.42	525	552	62.29
Chitosan-capped gold	0.47	522	559	71.99

Near-ultraviolet (NUV) radiation can be suppressed through proper capping. The highest NUV absorption is achieved when bare silica is used and gold NPs are capped with either polymer. The transmittance is reduced

to  $-7$  dB for 100 bi-layers. When films were formed with silica particles with chitosan or PDDA the NUV transmittance was found to increase to  $-4$  dB for 100 layers. When capping silica NPs, the absorption in the green-orange spectrum increases. The shade of the filter color is controlled by the film thickness.

#### Effect of the film thickness on filter transmittance

Here the effect of the film thickness on the transmission spectrum of the film, particularly the film color, is reported. The transmittance spectra of a film composed of alternating layers of chitosan-capped silica and gold NPs with different number of bi-layers are shown in Fig. 4. The transmittance is reduced in the UV, blue, and green regions of the spectrum. The two dips (peaks of absorption) correspond to absorption due to silica and gold NPs, respectively. Both dips decrease with different rates. The slope of reduction (when assumed linear) corresponds to the average absorption coefficient of the film at the two resonances. This is illustrated in Fig. 5a where the linear slope represents an exponential decay with absorption coefficients of  $1125$  and  $1397$  cm<sup>-1</sup> for the silica and gold resonances.

The film color (on transmittance) was estimated by calculating the RGB color value from the transmittance plots in Fig. 4. The wavelength of the red light was set at 650 nm, green at 510 nm, and blue at 475 nm. The transmittance for these three wavelengths was normalized to a maximum value of 255 and the result was an RGB color code of the film. Increasing the film thickness through the number of layers decreases the shades of each color with different slopes according to film absorption as shown in Fig. 5b. In this case, the slopes are 1.0, 1.5, and 1.8 shades per layer for red, green, and blue, respectively.

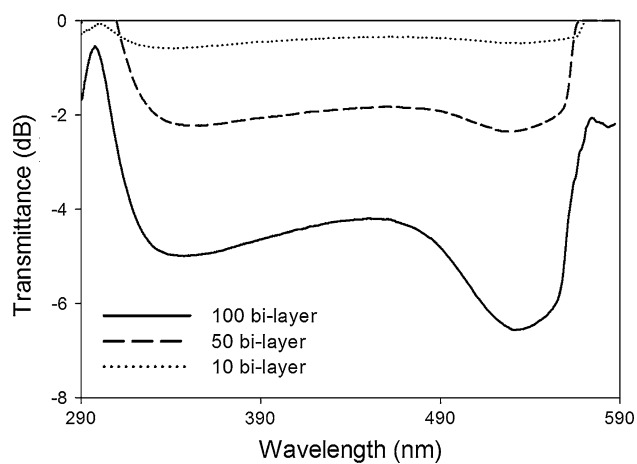


**Fig. 4** Transmittance of chitosan-capped silica and gold NPs for different number of layers: 10 layers (dotted), 50 layers (dashed), and 100 layers (solid)

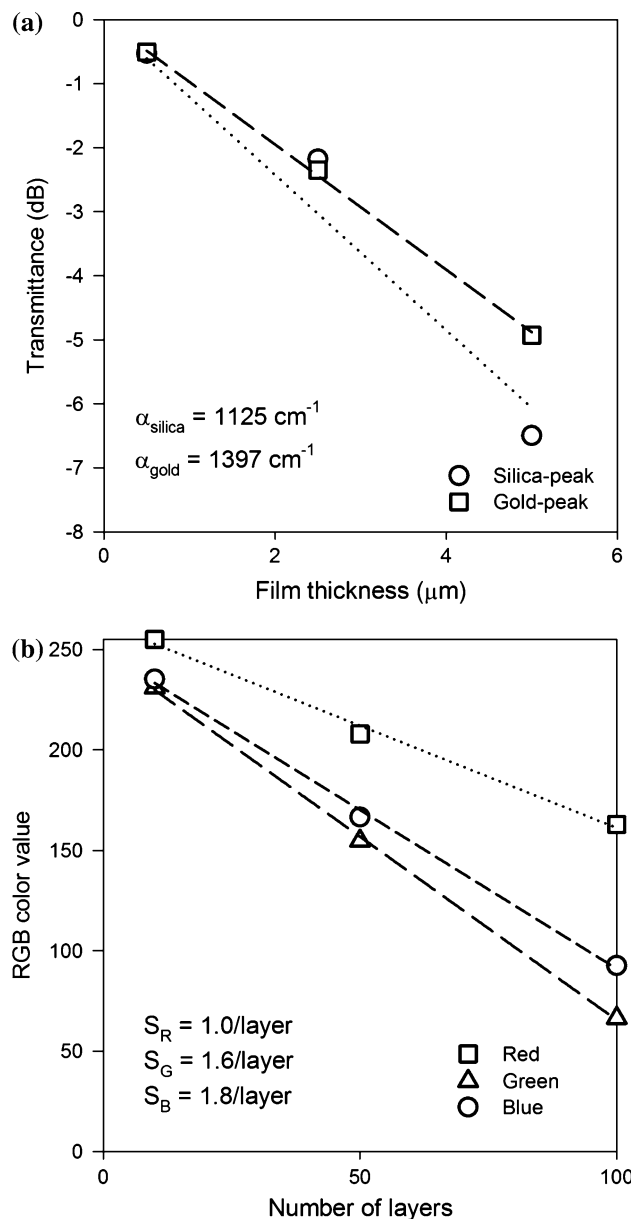


**Fig. 5** **a** Measured transmittance at the chitosan-gold (squares) and bare silica (circles) peak absorption. The linear fit (dashed and dotted lines) represents an exponential decay with constant absorption coefficients for silica and gold peaks. **b** Change of red (650 nm), green (510 nm), and blue (475 nm) color components with film thickness

In the proposed color filter, the color shade is controlled by the film thickness when proper capping is used (chitosan-capped silica in the example above). The slope of change of the green and blue components with the film thickness is almost similar. This is not the case of red where the slope is almost half that of green. For 10 bi-layered film, the transmitted color is very pale crimson (color code: #FAE6EB). Increasing the thickness to 50 and 100 layers changes the transmittance to colors of codes

#D09AA6 and #A2425D, respectively [41]. Those colors are very close to light crimson (standardized color distance of 7%) and moderate crimson (standardized color distance of 2%). The standardized color distance between two colors is defined as

$$\Delta C = (|R_1 - R_2| + |G_1 - G_2| + |B_1 - B_2|)/(3 \times 255) \quad (1)$$

R, G, and B are the red, green and blue color values, respectively. Increasing the film thickness by one layer causes a difference of the R, G, and B components by 1.0, 1.6, and 1.8, respectively. That corresponds to a color difference,  $\Delta C$ , of 0.6% calculated from Eq. 1. Hence, thicker film moves the transmittance to darker shades of crimson with a precision of 0.65% per added layer.

## Conclusions

A novel approach of implementing optical thin film filters based on layer-by-layer deposition is presented. The films were made by the self-assembly of oppositely charged metal and dielectric NPs, alternately capped with polymers. Synthesized colloidal suspensions of gold NPs ( $\sim 20 \text{ nm}$ ) and silica (Si) NPs ( $\sim 30 \text{ nm}$ ) were used as the building blocks for the self-organization of the films. Capping with PDDA and chitosan was used effectively to control the optical absorption of the surface plasmon resonance peaks of the gold NPs. Using different combinations of layer formation, absorption characteristics in the NUV, green and blue region were controlled through capping and varying the thickness of the film. Capping with chitosan or PDDA reduced the absorption peak of the coated silica NPs in a similar fashion. Peak absorption in the UV range was achieved by assembling bare silica NPs layers onto layers of gold NPs. Transmission color was controlled (less than 1% color distance per added bi-layer) by changing the film thickness.

**Acknowledgements** The authors would like to acknowledge partial financial support from the National Nanotechnology Center, belonging to the National Science & Technology Department Agency (NSTDA), Ministry of Science and Technology (MOST), Center of Excellence in Nanotechnology (CoEN), Asian Institute of Technology (AIT), Thailand and Higher Education Commission (HEC), Pakistan.

## References

- Shin D, Tibuleac S, Madonado TA, Magnusson R (1998) Opt Eng 37:2634
- Moreno I, Araiza JJ (2004) Proc Nov Opt Syst Design Optim VII 5524:409

3. Kurt P, Banerjee D, Cohen RE, Rubner MF (2009) *J Mater Chem* 19:8920
4. Liz-Marzán LM, Giersig M, Mulvaney P (1996) *Langmuir* 12:4329
5. Heavens OS (1986) *J Mod Opt* 33:1336
6. Hsiao CN, Chiu PK, Cho WH (2010) *Thin Solid Films* 518:7421
7. Tang CJ, Jaing CC, Wu K, Lee CC (2009) *Thin Solid Films* 517:1746
8. Affinito J, Martin P, Gross M, Coronado C, Greenwell E (1995) *Thin Solid Films* 270:43
9. Sagdeo PR, Shinde DD, Misal JS, Kamble NM, Tokas RB, Biswas A, Poswal AK, Thakur S, Bhattacharyya D, Sahoo NK, Sabharwal SC (2010) *J Phys D* 43:45302
10. Waldorf AJ, Dobrowolski JA, Sullivan BT, Plante LM (1993) *Optics* 32:5583
11. Dutta J, Hofmann H (2004) In: Nalwa HS (ed) *Encyclopedia of nanoscience and nanotechnology*. American Scientific Publisher, California, pp 617–640
12. Ni YX, Feng B, Wang J, Lu X, Qu S, Weng J (2009) *J Mater Sci* 44:4031. doi:[10.1007/s10853-009-3562-0](https://doi.org/10.1007/s10853-009-3562-0)
13. Promnimit S, Cavelius C, Mathur S, Dutta J (2008) *Physica E* 41:285
14. Schneider G, Decher G (2004) *Nano Lett* 4:1833
15. Hornyak GL, Tibbals HF, Dutta J (2009) *Introduction to nanoscience*. CRC Press, Florida, p 274
16. Ahn JS, Hammond PT, Rubner MF, Lee I (2005) *Colloid Surf A* 259:45
17. Kelly L, Coronado E, Zhao LL, Schatz GC (2003) *J Phys Chem B* 107:668
18. Guo N, DiBenedetto SA, Tewari P, Lanagan MT, Ratner MA, Marks TJ (2007) *Chem Mater* 22:1567
19. Noguez C (2007) *J Phys Chem C* 111:3806
20. Trachuk LA, Vrublevsky SA, Khlebtsov BN, Melnikov AG, Khlebtsov NG, Zimnyakov DA (2004) *Proc SPIE Int Soc Opt Eng* 5772:1
21. Perez-Gonzalez O, Zabala N, Borisov AG, Halas NJ, Nordlander P, Aizpurua J (2010) *Nano Lett* 10:3090
22. El-Sayed MA (2001) *Acc Chem Res* 34:257
23. Lin SY, Wu SH, Chen CH (2006) *Angew Chem Int Ed* 45:4948
24. Velikov KP, Blaaderen AV (2001) *Langmuir* 17:4779
25. Shipway AN, Katz E, Willner I (2000) *ChemPhysChem* 1:18
26. Sugunan A, Dutta J (2006) In: *Proceedings of materials research society symposium report #0901-Ra16-55-Rb16-55.1*
27. Arrascue ML, Garcia HM, Horna O, Guibal E (2003) *Hydro-metallurgy* 71:191
28. Liu Y, Wang Y, Claus RO (1998) *Chem Phys Lett* 298:315
29. Stöber W, Fink A, Bohn E (1968) *J Colloid Interface Sci* 26:62
30. Lvov Y, Ariga K, Onda M, Ichinose I, Kunitake T (1997) *Langmuir* 13:6195
31. Lan W, Li S, Xu J, Luo G (2010) *Biomed Microdevices* 12:1087
32. Jafri SHM, Dutta J, Sweatman D, Sharma AB (2006) *Appl Phys Lett* 89:133123-1
33. Bai Y, Zhao S, Zhang K, Sun C (2006) *Colloid Surf A* 281:105
34. Sugunan A, Thanachayanont C, Dutta J, Hilborn JG (2005) *Sci Technol Adv Mat* 6:335
35. Promnimit S, Jafri SHM, Sweatman D, Dutta J (2008) *J Nanoelectron Optoelectron* 3:184
36. Abid MI, Promnimit S, Dutta J (2008) In: *Proceedings of the 1st biannual NanoThailand Symposium (NTS)*, Bangkok, pp 321–322
37. Kooij ES, Brouwer EAM, Wormeester H, Poelsema B (2002) *Langmuir* 18:7677
38. Adamczyk Z, Weroński P, Barbasz J, Kolasińska M (2007) *Appl Surf Sci* 253:5776
39. El-Brolossy TA, Abdallah T, Mohamed MB, Abdallah S, Easawi K, Negm S, Talaat H (2008) *Eur Phys J Spec Top* 153:361
40. Nikolajsen T, Leosson K, Salakhutdinov I, Bozhevolnyi SI (2003) *Appl Phys Lett* 82:668
41. Frery AC, Melo CAS, Fernandes RC (2000) *Color Res Appl* 25:435